The ROYAL COLLEGE of OPHTHALMOLOGISTS

www.nature.com/eye

REVIEW ARTICLE

Check for updates

Anterior segment optical coherence tomography in ocular surface tumours and simulating lesions

Ahmet Kaan Gündüz[1,2]✉, Ibadulla Mirzayev[1,3], Aylin Okcu Heper[4], Işınsu Kuzu[4], Zarifakhanim Gahramanli[4], Cevriye Cansiz Ersöz[4], Ömür Özlenen Gündüz[1] and Ömür Ataoğlu[5]

This study aims to systematically review the reported literature on the use of anterior segment optical coherence tomography (AS-OCT) in ocular surface tumours and simulating lesions. A systematic literature search was done using PubMed, Scopus, and Web of Science databases between January 2002 and December 2021. On AS-OCT, ocular surface squamous neoplasia typically demonstrate epithelial thickening, epithelial hyperreflectivity, and an abrupt transition between normal and abnormal epithelium. Conjunctival nevi usually show mildly hyperreflective epithelium of normal thickness, internal hyperreflectivity, and intralesional cysts which is the hallmark of this tumour. Primary acquired melanosis presents with normal thickness epithelium, basal epithelial hyperreflectivity, and absence of cysts. Conjunctival melanoma demonstrates hyperreflective normal/thickened epithelium, hyperreflective basal epithelium, internal hyperreflectivity, and absence of intralesional cysts. Conjunctival lymphoma shows homogenous, low-medium reflective subepithelial lesions with smooth borders, and dot-like infiltrates. Benign reactive lymphoid hyperplasia findings are similar to lymphoma but the infiltrates are more hyperreflective compared to lymphoma. Pterygium shows thickened conjunctival epithelium, epithelial hyperreflectivity, and subepithelial wedge-shaped hyperreflective tissue separated from the overlying epithelium by a cleavage plane. Pinguecula demonstrates mildly thickened epithelium and similar findings with pterygium but does not extend beyond the corneal limbus. This review shows that AS-OCT, as a noninvasive tool, has potential uses in the differential diagnosis of ocular surface tumours and simulating lesions. Major limitations of AS-OCT include limited visualization of the posterior border of thick, keratinized, and pigmented tumours and lack of assessment of large conjunctival tumours in a single cut.

Eye (2023) 37:925–937; https://doi.org/10.1038/s41433-022-02339-1

I. INTRODUCTION

Ia. Classification of conjunctival tumours

Conjunctival tumours include a large spectrum of conditions ranging from benign to aggressive, life-threatening malignant tumours [1–6]. The most frequent benign conjunctival tumour is nevus followed by papilloma, primary acquired melanosis (PAM), and simple cysts [1, 2, 4, 5]. The most frequent malignant tumours of the ocular surface are ocular surface squamous neoplasia (OSSN), conjunctival melanoma, and conjunctival lymphoma (CL) [1, 2, 4, 5]. Conjunctival melanoma is the most common malignant tumour in some series and OSSN in others [1, 2]. Malignant conjunctival tumours may originate from benign/premalignant precursors. Distinguishing benign from malignant lesions can sometimes pose clinical difficulty. Early diagnosis is essential to reduce morbidity due to local treatment and cancer-related mortality. Conjunctival tumours can be conveniently classified as follows: (1) choristomas, (2) epithelial tumours, (3) melanocytic tumours, (4) vascular tumours, (5) myogenic tumours, (6) neural/xanthomatous/myxomatous/lipomatous tumours, (7) lymphoid and leukemic tumours, (8) lacrimal gland tumours, (9) caruncular tumours, (10) secondary tumours, (11) metastatic tumours, (12) inflammatory/infectious lesions, and (13) non-neoplastic masqueraders including degenerative lesions [1, 2, 7].

Ib. Optical coherence tomography: Basic principles and different types

Optical coherence tomography (OCT) is a non-invasive method that provides the opportunity to examine tissues by taking cross-sectional images. The operating principle of OCT is based on Michelson's low coherence interferometry [8, 9]. The interferometer splits the light beam into 2 paths, a reference path and a sampling path. The amplitude and phase delay of light reflected from tissues with different reflectivities are compared with the light reflected from the reference mirror [8]. In this way, a large number of interference patterns are obtained. A-scan images are generated by combining these interference patterns. Cross-sectional B-scan images are created from these A-scan images.

There are basically 3 types of OCT instruments: time-domain (TD), spectral-domain (SD), and swept-source (SS). TD-OCT uses a movable reference mirror while SD-OCT uses a fixed reference mirror. SD-OCT and SS-OCT systems use Fourier transformation analysis. The scanning speed of TD-OCT systems is low (400-2.000

[1]Department of Ophthalmology, Ankara University Faculty of Medicine, Ankara, Turkey. [2]Private Eye Clinic, Ankara, Turkey. [3]Department of Ophthalmology, Dünyagöz Hospital, Ankara, Turkey. [4]Department of Pathology, Ankara University Faculty of Medicine, Ankara, Turkey. [5]Private Mikro-Pat Pathology Laboratory, Ankara, Turkey.
✉email: drkaangunduz@gmail.com

Received: 11 June 2022 Revised: 26 October 2022 Accepted: 28 November 2022
Published online: 13 December 2022

A-scans/second) due to the limited mechanical cycle time of the reference mirror [10]. SD-OCT devices can obtain 26.000–70.000 A-scans/second [10, 11]. Due to the longer wavelength (1050 nm) employed and high scan speeds (100.000 A-scans/second), SS-OCT achieves greater penetration and allows better visualization of the internal tissue features [12, 13].

Ic. Anterior segment OCT

Izzat et al. published the first paper on in vivo imaging of anterior segment (AS) structures using OCT in 1994. [14]. The same group later published on the use of a hand-held prototype OCT instrument designed specifically for examining AS structures [15]. The first TD AS-OCT devices introduced into the market (Visante; Carl Zeiss Meditec and SLO, Heidelberg Engineering) received Food and Drug Administration (FDA) approval in 2005 and 2006 respectively. Therefore, there has been a delay for more than a decade between initial research and development of AS-OCT and its availability on the market.

The use of OCT for imaging ocular surface tumours has evolved from TD-OCT to SD-OCT and then to SS-OCT instruments providing better axial resolution, increased scanning speed leading to better and more detailed images. The current generation of SD and SS-OCT devices used to image the posterior segment can also acquire AS images. Therefore, procurement of a separate AS-OCT device may no longer be necessary. Summary of the features of various commercially available OCT systems for AS examination is given in Table 1.

Id. Normal conjunctival anatomy on AS-OCT

The layers of the conjunctiva show different brightness on AS-OCT (Fig. 1A, B). The conjunctiva is composed of epithelium and stroma. The conjunctival epithelium, which consists of well-organized cell layers, appears hyporeflective on AS-OCT due to less scattering of light. The stroma consists of lymphoid and fibrous layers. The fibrous layer includes the blood vessels, lymphatics, and nerves of the conjunctiva. The vessels and nerves appear as hyporeflective, round-shaped spaces. Because the stroma contains less-organized fibrous, adenoid, and vascular structures, it scatters the OCT light highly and displays a hyperreflective appearance. Tenon's capsule consists of collagen and smooth muscle fibres and has a high reflectivity similar to the conjunctival stroma. The horizontal rectus muscles appear variably hypo-hyperreflective with hyperreflective tendons. The episclera and sclera show hyporeflectivity and hyperreflectivity respectively [16].

Conjunctival thickness measurements have usually been made 3–5 mm from the temporal limbus or inferotemporal limbus. The reason for choosing inferotemporal quadrant was to minimize interference of pinguecula, extraocular muscles, and Tenon's capsule in conjunctival thickness measurements. On AS-OCT, the average conjunctival epithelial, stromal, and total thicknesses were measured as 42–45 µm, 198 µm, and 240 µm, respectively [17, 18]. In Chinese subjects, conjunctival epithelial thickness decreased after age 20 (from 42 to 39 µm) and remained at relatively low levels until age 60 (38–40 µm), followed by a sharp increase after age 60 (48 µm) [17]. Conjunctival stromal thickness was found to decrease throughout life (from 224 to 157 µm) [17]. Tenon's capsule appears to have slightly less thickness than the conjunctiva on AS-OCT measurements. It is difficult to define a precise demarcation line between the conjunctival stroma and Tenon's capsule. The mean Tenon's capsule thickness was measured as 210 µm in one study [19]. The average total conjunctiva/Tenon's capsule thickness was between 180 and 393 µm in different publications [16, 19–21]. The differences in thickness may depend on the measurement positions and the properties of OCT machines (TD vs SD vs SS). Conjunctiva/Tenon capsule thickness were found to decrease after age 50 years [16].

II. LITERATURE SEARCH

The literature search was done according to the preferred reporting items for systematic reviews [22, 23]. We conducted a systematic search of all published articles related to the use of AS-OCT in ocular surface tumours and mimicking lesions published between January 1, 2002 and December 1, 2021. Databases that were searched included PubMed, Scopus, and Web of Science. We searched for publications using the following search terms in various combinations: "optical coherence tomography", "anterior segment optical coherence tomography", "tumour", "anterior segment tumour", "conjunctival neoplasm", "corneal neoplasm", "ocular surface tumours", "conjunctival tumours", "congenital lesions", "epithelial tumours", "ocular surface squamous neoplasia", "squamous cell carcinoma", "intraepithelial neoplasia", "papilloma", "pseudoepitheliomatous hyperplasia", "melanocytic tumours", "nevus", "primary acquired melanosis", "melanoma", "vascular tumours", "lymphangiectasia", "lymphatic malformation", "capillary hemangioma", "arteriovenous malformation", "pyogenic granuloma", "lymphoid tumours", "lymphoma", "benign reactive lymphoid hyperplasia", "neural tumours", "neuroma", "schwannoma", "myxoid tumours", "myxoma", "lacrimal gland tumours", "oncocytoma", "fibrous tumours", "histiocytic tumours", "lipomatous tumours", "metastatic tumours", "simulating lesions", "pterygium", "pinguecula", and "pseudopterygium". Only studies published in English were included if they reported AS-OCT findings in conjunctival tumours and/or simulating lesions. Unpublished studies and meeting abstracts were not included. Initial screening of articles by title and abstract was performed independently by 2 authors (AKG and IM). Duplicates of the same paper and articles that did not meet the inclusion criteria were excluded. Subsequently, the full texts of the articles were evaluated and the publications that met the inclusion criteria were identified. The reference lists of the identified publications were also evaluated and relevant publications were included. A total of 67 studies (42 original articles and 25 case reports) were included in the final assessment.

This study aims to provide a systematic review of AS-OCT findings in ocular surface tumours and simulating lesions. In this systematic review, conjunctival tumours and simulating lesions have been classified into (1) epithelial tumours (Fig. 1C–H), (2) melanocytic tumours (Fig. 2), (3) vascular tumours (Fig. 3A–C), (4) lymphoid tumours (Fig. 4), (5) neural tumours (Fig. 3D–F), (6) myxoid tumours, (7) lacrimal gland tumours, and (8) simulating lesions (Fig. 5).

III. RESULTS

IIIa. Conjunctival tumours and simulating lesions

1. Conjunctival epithelial tumours. Tumours that can arise from squamous epithelium of the conjunctiva include OSSN, acanthosis, actinic keratosis, papilloma, keratoacanthoma, and conjunctival pseudoepitheliomatous hyperplasia (PEH) [1]. The most common among these tumours is OSSN [1, 2].

1a. OSSN: Ocular surface squamous neoplasia is a term used to describe pre-cancerous and cancerous epithelial lesions of the cornea and conjunctiva and includes conjunctival intraepithelial neoplasia (CIN), carcinoma in situ (CIS), and invasive squamous cell carcinoma (SCC) [24]. While histopathological examination is still the gold standard for OSSN, there has been interest in adjunctive diagnostic methods including impression cytology and vital dye staining (lissamine green, rose bengal, toluidine blue, and methylene blue) [25]. The disadvantage of impression cytology is that only superficial atypical cells can be evaluated. The vital dye staining method is also insufficient because benign lesions can also be stained with these dyes. Considering these shortcomings,

Table 1. Summary of features of various commercially available OCT systems used for anterior segment examination[†].

OCT type	Manufacturer	Measurement principle	Optical source	Axial resolution (µm)	Transverse resolution (µm)	Scan speed (A-scans per second)	Scan depth (mm)	Maximum scan width (mm)
Visante OCT*	Carl Zeiss Meditec, Dublin, CA	Time-domain	SLD 1310 nm	18	60	2000	6	16
Slit Lamp OCT*	Heidelberg Engineering, Heidelberg, Germany	Time-domain	SLD 1310 nm	<25	20–100	200	7	15
Cirrus OCT[§]	Carl Zeiss Meditec, Dublin, CA	Spectral-domain	SLD 840 nm	5[♯]	15[♯]	27.000	2	6
Stratus OCT[§]	Carl Zeiss Meditec	Time-domain	SLD 820 nm	10[♯]	20[♯]	400	2	N/A
Spectralis OCT[§]	Heidelberg Engineering, Heidelberg, Germany	Spectral-domain	SLD 820 nm	7[♯]	20[♯]	40.000	2	6
OCT SLO[§]	Optos	Spectral-domain	SLD 830 nm	<6[♯]	20[♯]	27.000	2	N/A
3D OCT 2000[§]	Topcon Corporation, Tokyo,Japan	Spectral-domain	SLD 840 nm	5–6[♯]	20[♯]	50.000	2.3	6
SOCT Copernicus[§]	Optopol	Spectral-domain	SLD 850 nm	3[♯]	12–18[♯]	52.000	2	10
Optovue iVue[§]	Optovue, Inc, Fremont, CA	Spectral-domain	SLD 840 nm	5[♯]	15[♯]	26.000–80.000**	2–2.3	13
Nidek RS 3000[§]	Nidek, Gamagori, Japan	Spectral-domain	SLD 880 nm	7[♯]	15[♯]	53.000	2	8
Revo NX[§]	Optopol, Zawiercie, Poland	Spectral-domain	SLD 830 nm	5[♯]	18[♯]	110.000	2.4	16
Anterion*	Heidelberg Engineering, Heidelberg, Germany	Swept-source	Swept-source laser 1300 nm	<10	<30	50.000	14	16.5
CASIA SS-1000 OCT*	Tomey Corporation, Nagoya, Japan	Swept-source	Swept-source laser 1310 nm	10	30	30.000	6	16
Triton OCT[§]	Topcon Corporation, Tokyo, Japan	Swept-source	Swept-source laser 1050 nm	8[♯]	20[♯]	100.000	3	3–12

OCT Optical coherence tomography, *SLD* Superluminescent light emitting diode, *N/A* Not available.

[†]Table adapted in part from Ang M, Baskaran M, Werkmeister RM, Chua J, Schmidl D, Aranha Dos Santos V, et al. Anterior segment optical coherence tomography. Prog Retin Eye Res 2018;66:132–156.

[♯]The quoted resolution values refer to posterior segment examination.

[§]Hybrid OCT device: for both anterior and posterior segment examination.

*For anterior segment examination only.

**The range refers to earlier and latest versions of the OCT equipment.

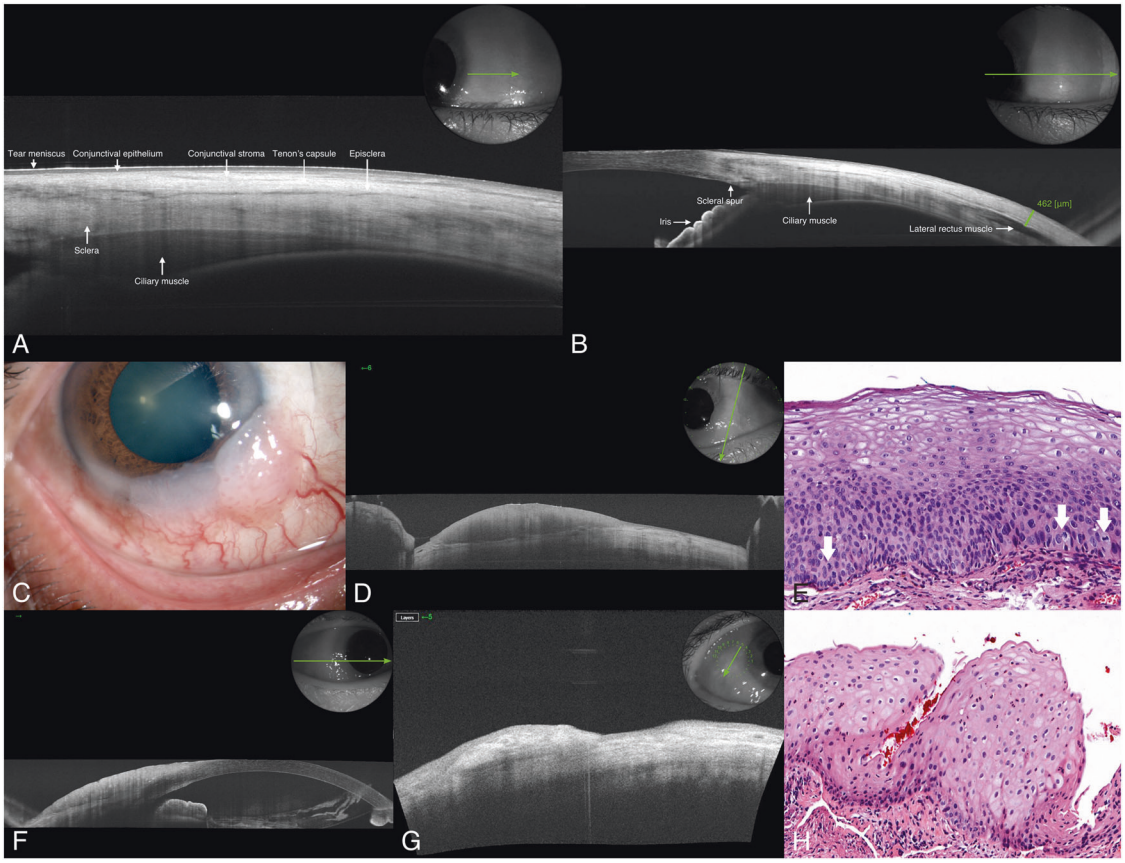

Fig. 1 Normal conjunctival anatomy (A, B), ocular surface squamous neoplasia (C–F), and conjunctival epithelial hyperplasia (G, H). **A** Anterior segment swept-source optical coherence tomography (AS SS-OCT) 6 mm line scan at the temporal limbus shows normal conjunctiva anatomy in a 10-year old male patient. The tear film appears hyperreflective and the underlying epithelium is hyporeflective. The conjunctival stroma and Tenon's capsule appear as hyperreflective structures. The hyporeflective interface between the two layers may represent conjunctival vessels and nerves in the fibrous layer of the stroma. The hyporeflective layer below Tenon's capsule probably represents episcleral vessels. The inset depicts the direction and location of the AS-OCT scan. **B** AS SS-OCT 16 mm line scan at the temporal quadrant of the same patient shows the conjunctiva and Tenon's capsule above the lateral rectus muscle. The combined thickness of the conjunctiva and Tenon's capsule is 462 µm. The sclera below is also hyperreflective compared to the rectus muscle. The ciliary muscle, scleral spur, and iris are also visible in this cut (arrows). The inset depicts the direction and location of the AS-OCT scan. **C** AS photograph of the left eye shows inferotemporally located gelatinous conjunctival intraepithelial neoplasia (CIN) overriding the limbus with corneal invasion. **D** AS SS-OCT image of the lesion in **C** depicts thickened (maximal epithelial thickness: 1060 µm) and hyperreflective epithelium with abrupt transition between normal and abnormal epithelium. Posterior shadowing due to the thick lesion is noted. The inset depicts the direction and location of the AS-OCT scan. **E** Histopathological examination after complete excision of the lesion in **C** demonstrates dysplastic squamous cells originating from the basal part of the epithelium and spreading at least the lower half of the epithelium. Suprabasal mitotic figures (arrows) accompany dysplastic cells. The integrity of the upper half of the epithelium is preserved (H&E x 25.2). **F** Another CIN lesion with thick (maximal epithelial thickness: 695 µm) and hyperreflective epithelium, high reflectivity, and abrupt transition from normal to abnormal epithelium. Image artifacts are visible. The inset depicts the direction and location of the AS-OCT scan. **G** AS SS-OCT image shows thickened (maximal epithelial thickness: 455 µm) and hyperreflective conjunctival epithelium. The inset depicts the direction and location of the AS-OCT scan. **H** Histopathological examination demonstrates keratinocytic proliferation and cytoplasmic clearing which is due to intracellular oedema of conjunctival squamous epithelium. There is an increase in conjunctival thickness. Features of atypia and dysplasia are absent. In addition, scattered neutrophils in the epithelium and mild mononuclear inflammatory cell infiltration are noted in substantia propria (H&E x 23.1).

there has been an increased interest in the use of AS imaging techniques including ultrasonic biomicroscopy (UBM), in-vivo confocal microscopy, and AS-OCT in the diagnosis of OSSN.

Three key characteristic AS-OCT findings of OSSN lesions are: (1) epithelial thickening; (2) epithelial hyperreflectivity; and (3) an abrupt transition between normal and abnormal epithelium (Fig. 1C–E) [26–49]. Epithelial hyperreflectivity, epithelial thickening, and abrupt transition between normal and abnormal epithelium were reported in 93%, 91%, and 81% of OSSN cases, respectively [34]. All 3 findings were found in 75%, any 2 in 23%, and one in 2% [34]. In thick lesions, shadowing of the underlying tissues may be observed [26, 27, 29]. Sensitivity and specificity of AS SD-OCT as a diagnostic method for detection of OSSN were reported as 93% and 70%, respectively [34]. Correlation of AS-OCT diagnosis with the histopathological diagnosis was found in 93% of OSSN lesions [34].

AS-OCT is useful in the diagnosis of OSSN patients who present with both classical and subtle clinical findings [30–32, 35]. In a study evaluating the ability of 34 novice clinicians to interpret AS-OCT for ocular surface lesions, the initial correct identification rate of OSSN lesions was 62% but this increased to 76% after a single 20-minute lecture on the interpretation of AS-OCT findings [35]. Some OSSN lesions with subtle findings were deemed as challenging to interpret by authors [35]. In these cases, the frequency of recognition was lower pre-lecture (55%) but still improved to 71% post-lecture [35].

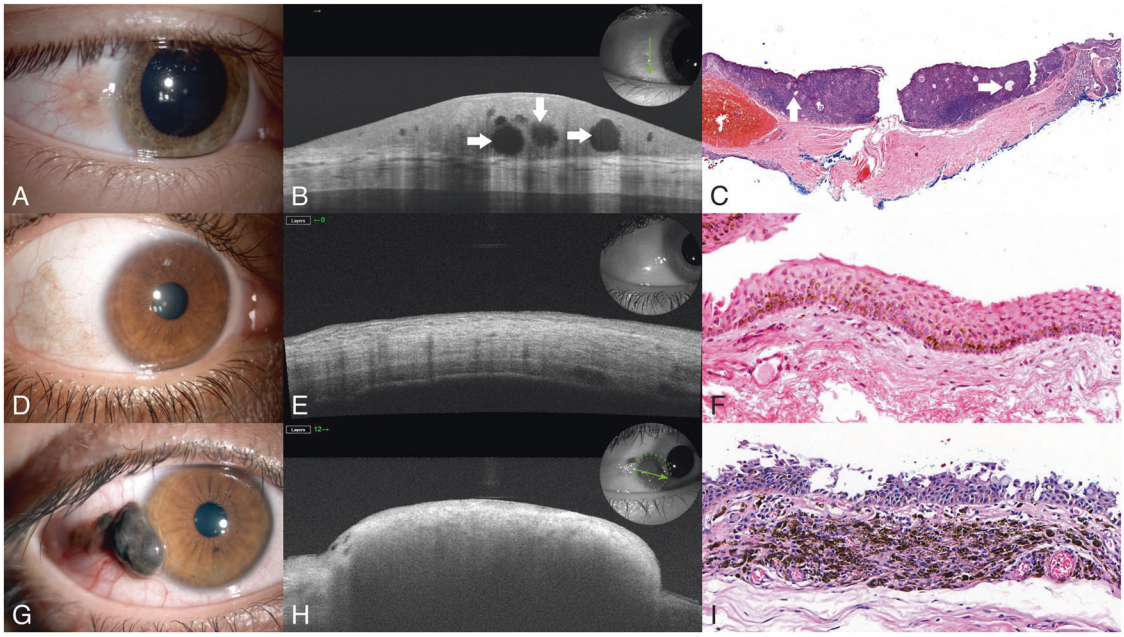

Fig. 2 Conjunctival melanocytic tumours including conjunctival nevus (A–C), primary acquired melanosis (PAM) (D–F), and conjunctival melanoma (G–I). A Anterior segment (AS) photograph of the right eye shows temporally located conjunctival nevus with intralesional cysts. **B** AS swept-source optical coherence tomography (SS-OCT) image shows a homogeneous solid lesion with mildly hyperreflective epithelium, high internal reflectivity, posterior shadowing, and intralesional cysts (arrows). The inset depicts the direction and location of the AS-OCT scan. **C** Histopathological examination demonstrates a well-delineated plaque-like lesion occupying the upper conjunctiva. Small cysts are noticed in the lesion consistent with AS SS-OCT appearance (arrows) (H&E x 3.9). **D** AS photograph of the right eye shows temporally located primary acquired melanosis. **E** AS SS-OCT image discloses normal thickness epithelium with hyperreflectivity of the basal epithelial layer. The inset depicts the direction and location of the AS-OCT scan. **F** Histopathological examination demonstrates a slightly thickened and heavily pigmented conjunctival squamous epithelium in which the melanin pigment is denser at the lower layers of the epithelium. Proliferation of melanocytes is absent (H&E x 29.3). **G** AS photograph of the right eye depicts temporally located conjunctival melanoma. **H** AS SS-OCT image demonstrates normal epithelium, hyperreflective basal epithelium, hyperreflective subepithelial mass with posterior shadowing, and absence of intralesional cysts. The inset depicts the direction and location of the AS-OCT scan. **I** Histopathological examination shows that the conjunctival epithelium is thickened by infiltration of moderately large pleomorphic cells, some of which have melanin pigment. In the substantia propria, there are also a few atypical melanocytic cells intermingled with heavily pigmented melanophages (H&E x 25.2).

CIN versus invasive SCC: Differentiation of CIN from invasive SCC still remains a challenge on AS-OCT. Previous studies reported demarcation line and hyperreflective basal membrane in CIN, and hyporeflective intratumoural spaces in invasive SCC. Singh et al. reported that a hyporeflective clear plane of separation or demarcation line from underlying tissue was observed in 90% of intraepithelial OSSN, whereas no clear plane was observed in any cases with SCC [33].

Singh et al. found hyperreflective basal membrane above the clear plane in 60% of intraepithelial OSSN and only in 14% of SCC [33]. None of the cases with intraepithelial OSSN demonstrated hyporeflective areas, whereas 57% of cases with SCC showed such areas [33]. However, Vempuluru et al. observed intralesional hyporeflective spaces not only in SCC but also in intraepithelial OSSN (60% and 27% of cases, respectively) [34]. On histopathology, hyperreflective basement membrane corresponded to the crowded basal layer of dysplastic cells along the intact thickened basement membrane and hyporeflective areas demonstrated a correlation with intraepithelial fibrovascular stromal pockets [33].

The role of AS-OCT in the differential diagnosis of OSSN: Ocular surface squamous neoplasia can be confused clinically with a variety of lesions including pterygium, pinguecula, conjunctival melanoma, and various disorders affecting the ocular surface. Kieval et al. reported the SD ultra-high-resolution (UHR) OCT findings in 34 cases with either OSSN or pterygium [41]. The authors could reliably distinguish pterygium from OSSN and there was a good correlation between the histopathologic and UHR OCT findings in all cases [41]. The average epithelial thickness was 346 µm and 101 µm in OSSN and pterygium respectively and this difference was statistically significant [41]. The sensitivity and specificity of UHR OCT for distinguishing OSSN and pterygium was 94% and 100%, respectively, with a cutoff value of 142 µm in their series [41]. Nanji et al. and Garcia et al. found 100% sensitivity and specificity of AS SD-OCT to distinguish between OSSN and pterygium using a cut-off value of 120 µm and 141 µm respectively [39, 46]. Figures 1D, F, 5B, D illustrate the difference in epithelial thickness between OSSN and pterygium/pinguecula.

The distinguishing AS-OCT features of OSSN from conjunctival melanoma are discussed in section 2c. Other ocular surface disorders where AS-OCT was used in distinguishing the lesions from OSSN included conjunctival amyloidosis, conjunctival histiocytosis, Salzmann's nodular degeneration, mucous membrane pemphigoid, and limbal stem cell deficiency [38–40, 43].

However, some ocular surface lesions may present with findings similar to OSSN on AS-OCT. Füst et al. reported 6 cases with OSSN-like AS SD-OCT findings. However, the pathological diagnoses proved to be other conjunctival and corneal lesions including papilloma, pinguecula with epithelial dysplasia, keratotic plaque, parakeratosis, and recurrent herpetic keratitis [48]. Therefore, while AS-OCT can differentiate OSSN from other simulating lesions in the majority of cases, there can be overlap between AS-OCT findings of OSSN and other lesions.

Further, several ocular surface pathologies including pterygium, pinguecula, Salzmann's nodular degeneration, corneal scar tissue, chronic ocular surface inflammation, chemical injury, and limbal stem cell deficiency may co-exist with OSSN causing difficulty in diagnosis. Atallah et al. evaluated 12 cases with known ocular

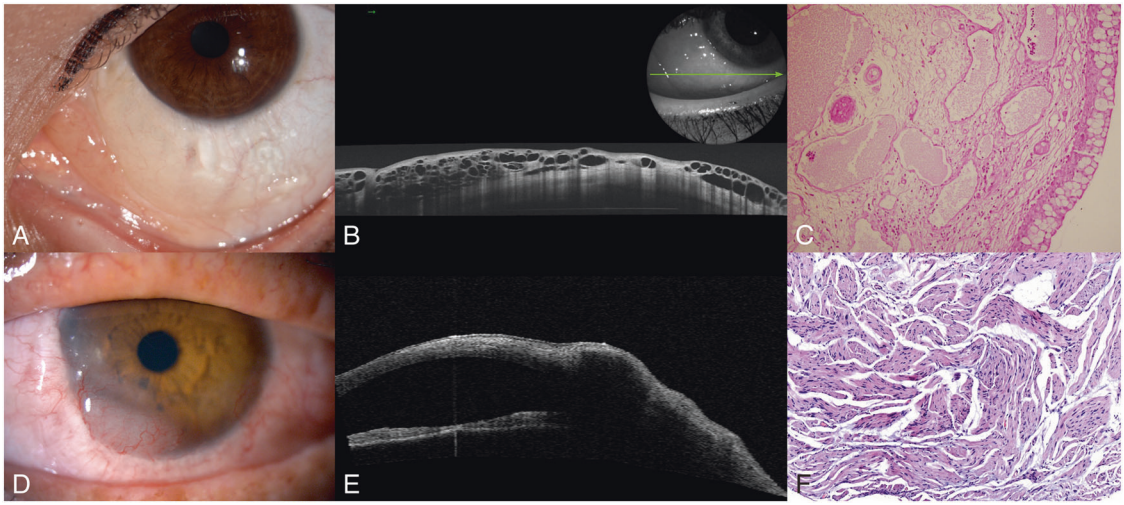

Fig. 3 Conjunctival lymphangioma (A–C) and conjunctival schwannoma (D–F). A Anterior segment (AS) photograph of the left eye depicts lymphatic cysts affecting the inferonasal conjunctiva in conjunctival lymphangioma. **B** AS swept-source optical coherence tomography (SS-OCT) image discloses dilated lymphatic channels manifesting as hyporeflective spaces with different sizes demarcated by hyperreflective septae. The inset depicts the direction and location of the AS-OCT scan. **C** Histopathological image demonstrates dilated lymphatic structures filled with lymphatic fluid and without any erythrocytes beneath the epithelium (H&E x 100). **D** AS photograph of the right eye shows corneal neovascularization and diffuse inferonasal perilimbal schwannoma. **E** Time domain AS-OCT image demonstrates a subepithelial localized mixed reflective irregular lobular mass. **F** Histopathological examination shows spindle cells in hypocellular short bundles with no atypia and mitosis consistent with schwannoma (H&E x 100).

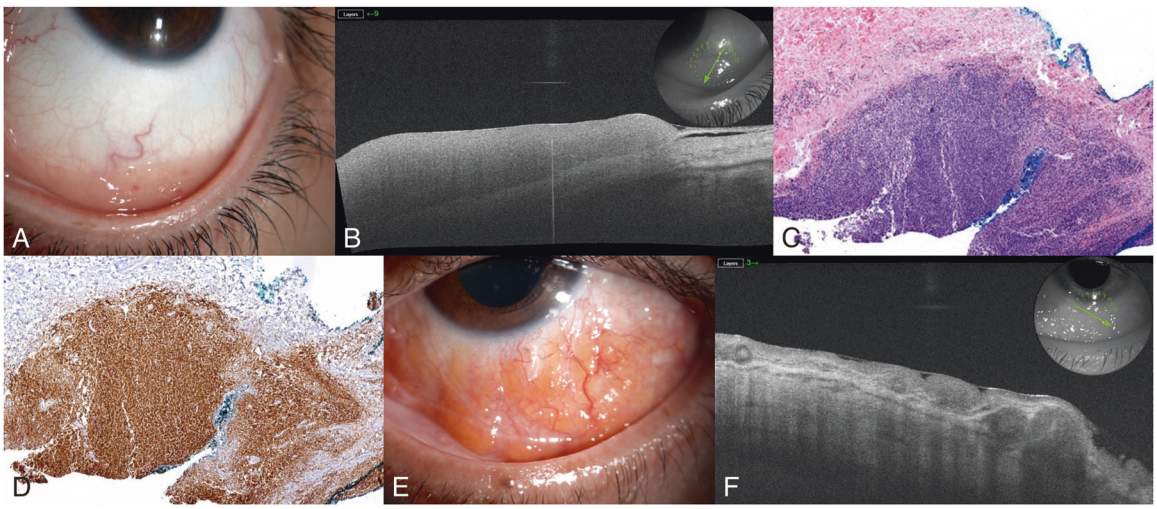

Fig. 4 Conjunctival lymphoid tumours including conjunctival lymphoma (A–D) and benign reactive lymphoid hyperplasia (E, F). A Anterior segment (AS) photograph of the left eye shows inferior salmon pink conjunctival lymphoma. **B** AS swept-source optical coherence tomography (SS-OCT) image demonstrates homogenous, medium reflective subepithelial lesion including multiple dot-like infiltrates. The inset depicts the direction and location of the AS-OCT scan. **C** Histopathological examination shows lymphoid infiltration of the conjunctiva (H&E x 0.9). **D** Immunohistochemical examination shows diffuse staining with CD20 (x 6.7). **E** AS photograph of the left eye depicts diffuse inferior conjunctival benign reactive lymphoid hyperplasia. **F** AS SS-OCT image discloses a subepithelial multilobular irregular mass. The inset depicts the direction and location of the AS-OCT scan.

surface diseases and co-existing OSSN [40]. The authors reported that 6 cases had limbal stem cell deficiency/scarring, 2 had rosacea, 2 had pterygium, one had pinguecula, and one had Salzmann's nodular degeneration in addition to OSSN [40].

AS-OCT-guided treatment in OSSN: In a study evaluating the standard of care of ophthalmologists who are likely to encounter OSSN, approximately half of the participants reported that they did not always perform a biopsy for suspected OSSN prior to initiation of topical chemotherapeutic agents [50]. Therefore, AS-OCT may be useful as a non-invasive auxiliary diagnostic method for the differential diagnosis of OSSN. The feasibility of providing in vitro optical biopsy for conjunctival tumours by AS-OCT and directing topical chemotherapy without the need for histopathologic confirmation is a rising trend.

Karp et al. imaged 8 OSSN eyes with UHR AS-OCT before excisional biopsy to determine the conjunctival margins of lesions. The data was transferred to a UHR AS-OCT device operating in conjunction with the operation microscope [44]. OSSN lesions subsequently underwent excisional biopsy and histologic tumour margins were compared with the AS-OCT predicted tumour borders. In all cases, the conjunctival tumour margins determined with the AS-OCT overlapped with the pathologically confirmed margins [44].

Tran et al. reviewed 95 cases of OSSN with clinically unapparent disease following topical 5-fluorouracil or interferon-alpha-2b and

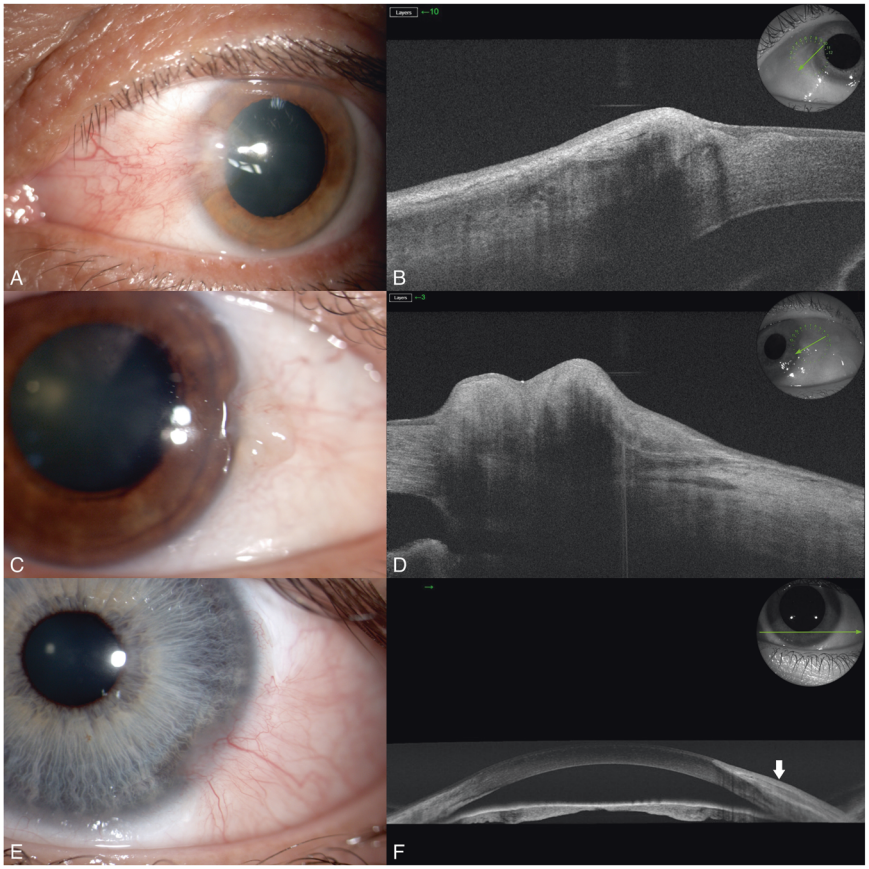

Fig. 5 Lesions simulating conjunctival tumours including pterygium (A, B), pinguecula (C, D), and pseudopterygium (E, F). A Anterior segment (AS) photograph of the left eye demonstrates nasally located conjunctival pterygium. **B** AS swept-source optical coherence tomography (SS-OCT) image of the left eye shows thickened (maximal epithelial thickness: 102 µm) conjunctival epithelium, epithelial hyperreflectivity, and subepithelial wedge-shaped hyperreflective tissue separated from the overlying epithelium by a cleavage plane. The inset depicts the direction and location of the AS-OCT scan. **C** AS photograph of the right eye demonstrates nasally located pinguecula. **D** AS SS-OCT image discloses slightly thickened (maximal epithelial thickness: 60 µm) and hyperreflective epithelium and subepithelial irregular hyperreflective tissue. The inset depicts the direction and location of the AS-OCT scan. **E** AS photograph of the left eye shows inferotemporally located flat pseudopterygium. **F** AS SS-OCT demonstrates flat hyperreflective lesion on the conjunctival and corneal epithelium (arrow). The AS-OCT features of this lesion are markedly different from pterygium depicted in **B**. The inset depicts the direction and location of the AS-OCT scan.

found subclinical OSSN with UHR AS-OCT in 17% of cases [31]. The authors concluded that UHR AS-OCT could identify residual subclinical disease in cases with clinically observed resolution [31].

Shousha et al. monitored lesion resolution using AS SD-OCT in 7 cases with OSSN [26]. Lesions were treated using topical interferon alfa-2b or 5-fluorouracil. In 4 cases, AS-OCT demonstrated normal epithelial features at clinical resolution. In 3 cases, on the other hand, AS-OCT demonstrated residual lesions manifesting as hyperreflective and thickened epithelium. Therapy was continued in these 3 cases and resulted in complete resolution of residual lesions on AS-OCT [26].

Sun and Hua investigated complete tumour regression using indocyanine green angiography (ICGA) and AS SD-OCT in 6 OSSN cases treated with subconjunctival/perilesional 5-fluorouracil [47]. The authors concluded that ICGA was better in detecting subtle recurrences but AS SD-OCT was good at determining treatment duration by preventing early cessation of topical treatment [47].

1b. Other epithelial tumours of the conjunctiva

Squamous papilloma: There are few studies on AS-OCT in conjunctival epithelial tumours other than OSSN. Vempuluru et al. found thickening of the epithelium, abrupt transition between normal and abnormal epithelium, and the presence of a cleavage zone between epithelium and stroma in 3 of 5 cases with squamous papilloma [34]. The authors emphasized the difficulty of differentiating squamous papilloma from OSSN using only AS SD-OCT [34]. Bolek et al. reported a case of conjunctival papilloma managed with AS SS-OCT-guided topical interferon alfa-2b and the authors found complete resolution after 3 months [51].

Pseudoepitheliomatous hyperplasia: Kaliki et al. evaluated AS SD-OCT findings of conjunctival PEH in 9 cases [52]. AS-OCT findings were irregular hyperreflective epithelium, epithelial dipping (down growth), and subepithelial hyperreflective lesion with posterior shadowing in all cases. There was no evidence of abrupt transition between normal and abnormal epithelium in any case [52]. Similarly, Vempuluru et al. detected epithelial dipping and did not observe abrupt transition between normal and abnormal epithelium in 3 PEH cases [34]. The authors also reported posterior shadowing in 2 cases and epithelial hyporeflectivity in one case [34]. In addition, they found intralesional cystic spaces in one lesion [34].

Conjunctival epithelial hyperplasia: Although there have been occasional case reports on conjunctival epithelial hyperplasia as a pathological entity, this lesion has not been sufficiently identified. A recent report highlighted the clinical and pathological features of conjunctival epithelial hyperplasia [53]. The lesion usually appears as a yellow conjunctival elevation mimicking other benign and malignant tumours. On AS-OCT, thickened and hyperreflective conjunctival epithelium are observed (Fig. 1F, G).

2. Conjunctival melanocytic tumours. Tumours that arise from the melanocytes of the conjunctiva include nevus (Fig. 2A–C), PAM (Fig. 2D–F), conjunctival melanoma (Fig. 2G–I), and racial melanosis. Ocular melanocytosis represents accumulation of melanocytes in the sclera and can mimic conjunctival melanocytic lesions [54]. Conjunctival nevus, PAM without atypia, and PAM with atypia carry nearly 1%, 0%, and 50% risk for transformation into malignant melanoma, respectively [55, 56]. Conjunctival melanoma can develop from PAM (57%), conjunctival nevus (4%), and de novo (39%) [57]. Considering the risk of metastatic disease and death from conjunctival melanoma, differentiation of this lesion from other conjunctival tumours is of utmost importance [58]. AS-OCT has recently been widely used in the diagnosis of conjunctival melanocytic tumours [59–65].

2a. Conjunctival nevus: Conjunctival nevi present as homogeneous and solid lesions with mildly hyperreflective epithelium of normal thickness in most cases on AS-OCT [39, 59, 60]. Visualization of anterior, posterior, and lateral margins was possible in 100%, 82–89.4%, and 86–96.5% of the cases [58, 61]. When compared with histopathology, AS TD-OCT was found to detect intrinsic cysts with a sensitivity of 80% and a specificity of 100% [59]. In almost all cases, a cleavage zone is observed between the epithelium and the stroma [34]. Shadowing is found especially in pigmented lesions [59]. Underlying sclera may not be seen in heavily pigmented lesions [62].

Histopathologically, conjunctival nevi are classified as compound (80%), subepithelial (15%), and junctional (5%) [66]. The presence of multiple intralesional hyporeflective cysts is an important diagnostic feature of conjunctival nevus on AS-OCT. Some cysts may feature hyperreflective material, probably representing desquamated epithelium and debris [54]. In a study evaluating diagnostic value of SD-OCT and UBM in conjunctival nevi, AS-OCT found to be superior in the detection of intralesional cysts (57.1% vs. 28.5%), while UBM was more precise in the visualization of the posterior margin (100% vs. 85.7%) [61]. In this study, conjunctival epithelial layer could be measured only in subepithelial nevi, while conjunctival epithelium could not be detected in junctional and compound nevi on AS-OCT [61].

2b. Conjunctival PAM: The largest series evaluating AS SD-OCT findings in PAM was reported by Alzahrani et al. [64]. The authors observed a uniformly thick basal epithelial hyperreflective band with normal thickness of the overlying epithelium and the absence of cysts in all 24 PAM cases on AS-OCT. Shadowing was found in 25% of cases. It was not possible to differentiate cases of PAM with atypia from those without atypia by AS SD-OCT [43, 64]. In one case of PAM with atypia, an atypical melanocytic nest was detected on pathological examination but this case also demonstrated a similar view to PAM without atypia on AS SD-OCT [64]. Nanji et al. observed that epithelial hyperreflectivity in PAM was easiest to appreciate when pigment was present on the cornea because the corneal epithelium is innately hyporeflective and provides greater contrast [39]. In this study, histopathology of PAM demonstrated a correlation between the atypical melanocytes detected within the basal epithelium of the conjunctiva and hyperreflectivity of the basal epithelium observed on AS SD-OCT [39].

2c. Conjunctival melanoma: Anterior segment OCT findings of conjunctival melanomas included hyperreflective epithelium with variable thickening, hyperreflective basal epithelium, and hyperreflective subepithelial mass [39, 65]. However, Shousha et al. reported normal thickness epithelium in 5 amelanotic melanoma cases in their series [43]. Posterior shadowing was detected especially in the pigmented and thick melanomas [39]. Unlike nevi, conjunctival melanomas did not demonstrate cysts on AS SD-OCT [39, 43, 65]. The presence of epithelial cleavage foci which indicates involvement of the epithelium with atypical melanocytes has also been reported in conjunctival melanoma [43].

Some cases of conjunctival amelanotic melanoma may clinically simulate OSSN [39, 43]. Normal or mildly increased epithelial thickness and the presence of a subepithelial lesion in amelanotic melanoma are important findings in the differential diagnosis from OSSN on AS SD-OCT [39, 43]. The presence of epithelial cleavage foci may also help to differentiate amelanotic melanoma from OSSN [43].

3. Vascular tumours

3a. Lymphangiectasia: Many AS-OCT studies on lymphangiectasia demonstrated a well-demarcated lesion with fluid spaces separated by thin septate walls (Fig. 3A–C) [67–75]. AS-OCT findings can also be used to plan the biopsy site and monitor treatment outcomes in conjunctival lymphangiectasia [71–74].

3b. Lymphatic malformation: Bekdemir et al. reported a case of conjunctival lymphatic malformation associated with orbital and mid-face vascular malformations [76]. The authors reported that the lymphatic malformation in their case had variable-sized interconnected hyporeflective spaces separated by hyperreflective tissue on AS SS-OCT in contrast to the fewer slit-like, slender, and fusiform appearing cysts seen in lymphangiectasia [75, 76].

3c. Capillary haemangioma and conjunctival arteriovenous malformation: Vempuluru et al. reported hyperreflective thick epithelium, zone of cleavage between epithelium and stroma, posterior shadowing, and no abrupt transition between normal and abnormal epithelium in capillary haemangioma and hyporeflective epithelium with normal thickness, the presence of cysts, zone of cleavage between epithelium and stroma, posterior shadowing, and no abrupt transition between normal and abnormal epithelium in arteriovenous malformation on AS SD-OCT [34]. Bradfield et al. reported a case of capillary haemangioma presenting as a scleral vascular lesion [77]. AS-OCT images of this case demonstrated multiple vessels within the mass and no capsule around the lesion [77].

3d. Pyogenic granuloma: The term pyogenic granuloma is actually a misnomer because the lesion is neither pyogenic nor granulomatous. It actually represents granulation tissue and risk factors for its development include suture material, trauma, pregnancy, and medications. There are few case reports describing AS-OCT findings in pyogenic granuloma developing after scleral buckle surgery and intravitreal injections [78–80]. AS-OCT in these cases showed a subepithelial hyperreflective mass with back shadowing and no abrupt transition from normal to abnormal epithelium.

4. Lymphoid tumours. Conjunctival lymphoma and benign reactive lymphoid hyperplasia (BRLH) usually demonstrate a clinically similar appearance although the clinical course of the former differs because of its malignant potential. Venkateswaran et al. compared the AS SD-OCT findings of CL (20 eyes) and BRLH (6 eyes) [81]. The conjunctival epithelium was normal in all CL and BRLH cases. In lymphoma, UHR AS-OCT demonstrated homogenous, dark subepithelial lesions with smooth borders, with monomorphic dot-like infiltrates (Fig. 4A–D). AS-OCT findings of BRLH were similar to lymphoma (Fig. 4E, F). However, monomorphic infiltrates were more hyperreflective in BRLH compared to lymphoma. A multilobular appearance with overlying tear film bridging the lobules may sometimes be seen in both types of lymphoid tumours. Histopathological examination revealed that BRLH lesions with reflectivity similar to lymphoma on AS-OCT were hypercellular, while more hyperreflective BRLH lesions were paucicellular. The authors noted that flow cytometry and gene rearrangement studies were needed for the final differentiation of these tumours [81]. Similar AS SD-OCT findings in CL and BRLH lesions were reported in several other studies [34, 39, 43, 82, 83].

5. Neural tumours. Neuroma and schwannoma are rare conjunctival neural tumours [1, 2]. Similar AS-OCT features were reported for these tumours including regular and normal thickness epithelium with a subepithelial mixed reflective irregular lobular mass (Fig. 3D–F) [84, 85]. Therefore, histopathological examination is mandatory for differentiating these lesions.

6. Myxoid tumours

Myxoma: Conjunctival myxoma is a rare, benign stromal tumour that may resemble a conjunctival cyst [86]. Alvarado-Villacorta et al. recently reported 2 cases presenting with a clinical diagnosis of conjunctival cyst which proved to be conjunctival myxoma at histopathological examination [86]. AS SD-OCT depicted a normal/mildly thickened conjunctival epithelium, subepithelial heterogeneous lesion with hypo- and hyperreflective areas lined by a highly hyperreflective band, and posterior shadowing [86].

7. Lacrimal gland tumours

Oncocytoma: Conjunctival oncyocytoma is a rare tumour and usually occurs in the caruncle. Based on its cytokeratin profile, it probably originates from lacrimal and accessory lacrimal gland cells [87]. AS-OCT disclosed a mixed solid and cystic lesion in 2 cases with oncocytoma located in bulbar conjunctiva (1 case) and caruncle (1 case) [88].

8. Lesions simulating conjunctival tumours

8a. Pterygium and pseudopterygium: Anterior segment SD-OCT findings in pterygium included variably thickened epithelium and subepithelial wedge-shaped hyperreflective tissue separated from the overlying epithelium by a cleavage plane [39, 41–43, 89–91]. The thickened epithelium is often hyporeflective; however, some hyperreflective epithelial areas can be observed, representing actinic changes (Fig. 5A, B) [41]. Pterygium attached to the cornea usually remains between the corneal epithelium and Bowman's layer [43]. Hyporeflective areas also may be detected in the subepithelial tissue that could represent blood vessels in the pterygium tissue [41].

Soliman et al. reported that recurrent pterygium lesions show an irregular mass with multiple humps and cystic changes compared to the smooth well-defined appearance of primary pterygium [89]. In addition, the authors reported that in pseudoterygium, the overgrowing membrane was actually not attached to the underlying epithelium and there was a cleavage plane between the lesion and the epithelium (Fig. 5E, F) [89].

Pujol et al. reported AS SD-OCT findings after pterygium surgery [92]. Cases with and without recurrence after excision were evaluated in 2 separate groups [92]. Identification of the corneal epithelium, both corneal and conjunctival epithelium, and limbal demarcation areas were more frequent in the no recurrence group compared to the recurrence group at 1 month, 3 months, and 6 months respectively [92].

There are also studies investigating the correlation between corneal aberrations and AS-OCT findings of pterygium. The horizontal length of the pterygium, reduced thickness of the head of the pterygium, limbal thickness, and the presence of flat bridging corneoscleral transition zone were significantly associated with increasing corneal astigmatism [93, 94]. While increasing pterygium size affected the raise of coma-like, spherical-like, and total higher-order aberrations, there was no correlation between spherical aberration and pterygium size [95].

8b. Pinguecula: Anterior segment OCT features of the pinguecula included normal to slightly thickened epithelium, mild conjunctival epithelial hyperreflectivity, and a wedge-shaped dark subepithelial mass close to the limbus [39, 89, 96, 97]. Pinguecula lesions typically do not extend over the corneal limbus (Fig. 5C, D).

8c. Amyloidosis: Conjunctival amyloidosis can be confused clinically with lymphoma. AS-OCT findings are important in the differential diagnosis. AS SD-OCT of amyloidosis demonstrated normal epithelium, heterogeneous subepithelial lesion with irregular borders, usually containing hyperreflective linear infiltrates [43, 81]. In lymphoma, homogeneity of the mass, smooth borders, and the presence of dot-like infiltrates were important findings in the differential diagnosis from amyloidosis on AS SD-OCT [39, 43, 81].

IIIb. SS-OCT versus SD-OCT in conjunctival tumours

Swept-source OCT features longer wavelength light at 1050 nm which is capable of deeper tissue penetration. Combined with its high scanning speed of 100.000 A scan/sec, SS-OCT is theoretically able to reveal more details compared to SD-OCT. However, axial resolution is less than SD-OCT which may result in loss of some tissue details.

There is only one paper comparing SS-OCT vs SD-OCT imaging findings in conjunctival tumours. The authors performed SS-OCT vs SD-OCT imaging in 11 isolated bulbar lesions of the conjunctiva or caruncle [98]. Detection of basement membrane and visualization of posterior tumour margins were possible with SS-OCT more frequently than with SD-OCT. The internal pattern of tumours demonstrated more heterogeneity with SS-OCT imaging. Tumour shadowing resulting from the imaging technique was milder and overall image quality was higher with SS-OCT than with SD-OCT [98].

IIIc. AS-OCT versus UBM in conjunctival tumours

Bianciotto et al. reported that TD-OCT and UBM were equally good for imaging conjunctival lesions [99]. Lauwers et al. found good correlation between thickness measurements of ocular surface tumours using AS SD-OCT and UBM [100]. AS SD-OCT provided better tumour details compared to UBM. However, AS-OCT was limited in imaging the posterior boundary of the tumour, especially in malignant and pigmented tumours [100]. Janssens et al. conducted a systematic review to determine the role of AS-OCT and UBM in ocular surface tumours [101]. The authors reached the following conclusions: (1) The disadvantage of AS-OCT is that it cannot penetrate deeper than 1–3 mm and cannot pass through pigmented lesions. (2) However, for smaller lesions, AS-OCT is a more accurate technique that can provide detailed images of the remaining healthy cornea, identify cysts, or be useful in detecting tumour recurrence. (3) For larger or pigmented lesions, UBM can better define tumour boundaries and tumour thickness [101]. AS-OCT can not penetrate the iris pigment epithelium and therefore, can not show tumours located posterior to this plane including ciliary body masses.

IV. CONCLUSIONS

Recently, AS-OCT has been widely used in the diagnosis of ocular surface tumours providing in vitro "optical biopsy" features (Table 2). The main AS-OCT findings in conjunctival lesions reported in the literature so far included thickened hyperreflective epithelium with abrupt transition from normal to abnormal tissue in OSSN as compared to a less thick epithelium in pterygium; high internal reflectivity and the presence of intratumoural cysts in conjunctival nevi as compared to high reflectivity but no cysts in conjunctival melanomas; dot-like infiltrates and medium reflectivity in conjunctival lymphoid lesions; and the presence of clear spaces divided by septae in lymphatic malformations.

Swept-source OCT offers deeper penetration and better image quality compared to SD-OCT [98]. Compared to UBM, AS-OCT offers similar if not better results in demonstrating internal tumour features [101]. However, UBM can better define tumour boundaries and tumour thickness in larger or pigmented ocular

Table 2. Anterior segment optical coherence tomography findings in ocular surface tumours and simulating lesions.

Conjunctival tumour	Anterior segment optical coherence tomography findings
Epithelial tumours	
Ocular surface squamous neoplasia	Epithelial thickening, epithelial hyperreflectivity, and an abrupt transition between normal and abnormal epithelium
Intraepithelial	Clear tissue plane between the underlying tissues and hyperreflective basal membrane
Invasive	Intralesional hyporeflective spaces
Squamous papilloma	Epithelial thickening, epithelial hyperreflectivity, and an abrupt transition between normal and abnormal epithelium
Pseudoepitheliomatous hyperplasia	Irregular hyperreflective epithelium, epithelial dipping (down growth), and subepithelial hyperreflective lesion
Melanocytic tumours	
Nevus	Mildly hyperreflective epithelium of normal thickness, homogeneous solid lesion with internal hyperreflectivity, and intralesional cysts
Primary acquired melanosis	Uniformly thick basal epithelial hyperreflective band with normal thickness of the overlying epithelium and the absence of intralesional cysts
Melanoma	Normal or mildly thickened hyperreflective epithelium, hyperreflective basal epithelium, internal hyperreflectivity, and absence of intralesional cysts
Vascular tumours	
Lymphangiectasia	Well-demarcated lesion with slender shaped fluid spaces separated by thin septate walls
Lymphatic malformation	Interconnected round-oval hyporeflective spaces demarcated by hyperreflective septae
Capillary haemangioma	Hyperreflective thick epithelium, zone of cleavage between epithelium and stroma, multiple vessels within the mass with no capsule, and posterior shadowing
Arteriovenous malformation	Hyporeflective normal thickness epithelium, the presence of cysts, zone of cleavage between epithelium and stroma, and posterior shadowing
Pyogenic granuloma	Subepithelial hyperreflective mass with posterior shadowing and no abrupt transition from normal to abnormal epithelium
Lymphoid tumours	
Lymphoma	Normal thickness epithelium, homogenous, hyporeflective subepithelial lesion with smooth borders, and monomorphic dot-like infiltrates
Benign reactive lymphoid hyperplasia (BRLH)	Similar findings with lymphoma; monomorphic infiltrates more hyperreflective in BRLH compared to lymphoma. Paucicellular lesions more hyperreflective and hypercelullar lesions similar in reflectivity to lymphoma
Neural tumours	
Neuroma	Normal thickness epithelium with a subepithelial mixed reflective irregular lobular mass
Schwannoma	Similar findings with neuroma
Myxomatous tumours	
Myxoma	Normal/mildly thickened conjunctival epithelium, subepithelial heterogeneous lesion with hypo- and hypereflective areas lined by a highly hyperreflective band, and posterior shadowing
Lacrimal gland tumours	
Oncocytoma	Mixed solid and cystic lesion
Histiocytic tumours	
Histiocytosis	Normal epithelium, subepithelial mass with small dots representing cellular infiltration, and hyporeflective areas representing blood vessels
Lesions simulating conjunctival tumours	
Pterygium	Thickened epithelium, hyperreflective epithelial areas (actinic changes?), and subepithelial wedge-shaped hyperreflective tissue separated from the overlying epithelium by a cleavage plane.
Pseudopterygium	Overgrowing membrane loosely attached to the underlying epithelium; cleavage plane between the lesion and the epithelium
Pinguecula	Normal to slightly thickened epithelium with mild epithelial hyperreflectivity and wedge-shaped hyporeflective subepithelial mass close to the limbus
Amyloidosis	Normal epithelium, heterogeneous subepithelial lesion with irregular borders usually containing hyperreflective linear infiltrates

surface lesions and in lesions located posterior to the iris pigment epithelium in case of iridociliary masses [101].

There are certain limitations for the use of AS-OCT in ocular surface tumours. First, leukoplakic, thick, and pigmented lesions can obscure details of underlying tissues. Second, AS-OCT can not show large conjunctival lesions in a single cut. Third, AS-OCT can not yet make a clear distinction between invasive and intraepithelial variants of OSSN. Fourth, there may still be overlapping features between OSSN and other conjunctival lesions including squamous papilloma, pinguecula with epithelial dysplasia,

keratotic plaque, and parakeratosis. Fifth, no definite distinguishing AS-OCT features have been reported for relatively rare tumours including vascular and neural tumours, oncocytoma, myxoma, and histiocytoma. In recent years, AS-OCT has proved to be an indispensable diagnostic tool in the diagnosis and management of conjunctival and corneal pathologies. Further developments in the optic resolution features of AS-OCT machines and use of artificial intelligence deep learning algorithms may improve the diagnostic capability of upcoming AS-OCT platforms.

REFERENCES

1. Shields CL, Alset AE, Boal NS, Casey MG, Knapp AN, Sugarman JA, et al. Conjunctival tumours in 5002 cases. Comparative analysis of benign versus malignant counterparts. The 2016 James D. Allen lecture. Am J Ophthalmol. 2017;173:106–33.
2. Mirzayev I, Gündüz AK, Gündüz ÖÖ, Özalp Ateş FS, Nalcı Baytaroğlu H. Demographic and clinical features of conjunctival tumours at a tertiary care centre. Clin Exp Optom. 2021;7:1–7.
3. Shields CL, Sioufi K, Alset AE, Boal NS, Casey MG, Knapp AN, et al. Clinical features differentiating benign from malignant conjunctival tumours in children. JAMA Ophthalmol. 2017;135:215–24.
4. Pellerano F, Gil G, Rosario A, Mañon N, Vargas T, Vizcaíno G. Survey of 138 Conjunctival tumors in the Dominican Republic. Ophthalmic Epidemiol. 2020;27:278–82.
5. García Onrubia L, Pacheco-Callirgos GE, Portero-Benito A, García-Álvarez C, Carreño Salas E, Muñoz-Moreno MF, et al. Spectrum of conjunctival tumours in a Spanish series: A review of 462 cases. Eur J Ophthalmol. 2020;30:1403–9.
6. Mirzayev I, Gündüz AK, Özalp Ateş FS, Özcan G, Işık MU. Factors affecting recurrence after surgical treatment in cases with ocular surface squamous neoplasia. Int J Ophthalmol. 2019;12:1426–31.
7. Rao R, Shields CL. Overview and classification of conjunctival and corneal tumors. In: Chaugule SS, Honavar SG, Finger PT, editors. Surgical Ophthalmic Oncology Cham, Germany: Springer; 2019. 69–74.
8. Michelson AA. The relative motion of the Earth and the luminiferous Ether. Am J Sci. 1881;22:120.
9. Huang D, Swanson EA, Lin CP, Schuman JS, Stinson WG, Chang W, et al. Optical coherence tomography. Science 1991;254:1178–81.
10. Ramos JL, Li Y, Huang D. Clinical and research applications of anterior segment optical coherence tomography - a review. Clin Exp Ophthalmol. 2009;37:81–9.
11. Mavadia-Shukla J, Fathi P, Liang W, Wu S, Sears C, Li X. High-speed, ultra high-resolution distal scanning OCT endoscopy at 800 nm for in vivo imaging of colon tumorigenesis on murine models. Biomed Opt Express. 2018;9:3731–9.
12. Stanga PE, Tsamis E, Papayannis A, Stringa F, Cole T, Jalil A. Swept-source optical coherence tomography angio™ (Topcon Corp, Japan): Technology review. Dev Ophthalmol. 2016;56:13–17.
13. Ang M, Baskaran M, Werkmeister RM, Chua J, Schmidl D, Aranha Dos Santos V, et al. Anterior segment optical coherence tomography. Prog Retin Eye Res. 2018;66:132–56.
14. Izatt JA, Hee MR, Swanson EA, Lin CP, Huang D, Schuman JS, et al. Micrometer-scale resolution imaging of the anterior eye in vivo with optical coherence tomography. Arch Ophthalmol. 1994;112:1584–9.
15. Radhakrishnan S, Rollins AM, Roth JE, Yazdanfar S, Westphal V, Bardenstein DS, et al. Real-time optical coherence tomography of the anterior segment at 1310 nm. Arch Ophthalmol. 2001;119:1179–85.
16. Fernández-Vigo JI, Shi H, Burgos-Blasco B, De-Pablo-Gómez-de-Liaño L, Almorín-Fernández-Vigo I, Kudsieh B, et al. Impact of age, sex and refractive error on conjunctival and Tenon's capsule thickness dimensions by swept-source optical coherence tomography in a large population. Int Ophthalmol. 2021;41:3687–98.
17. Zhang X, Li Q, Xiang M, Zou H, Liu B, Zhou H, et al. Bulbar conjunctival thickness measurements with optical coherence tomography in healthy Chinese subjects. Invest Ophthalmol Vis Sci. 2013;54:4705–9.
18. Feng Y, Simpson TL. Corneal, limbal, and conjunctival epithelial thickness from optical coherence tomography. Optom Vis Sci. 2008;85:E880–3.
19. Kumar DA, Agarwal A, Karnathi S, Patadiya R. Anterior segment optical coherence tomography for imaging the sub-Tenon space. Ophthalmic Res. 2013;50:231–4.
20. Salcedo-Villanueva G, Paciuc-Beja M, Harasawa M, Velez-Montoya R, Olson JL, Oliver SC, et al. Identification and biometry of horizontal extraocular muscle tendons using optical coherence tomography. Graefes Arch Clin Exp Ophthalmol. 2015;253:477–85.
21. Howlett J, Vahdani K, Rossiter J. Bulbar conjunctival and Tenon's layer thickness measurement using optical coherence tomography. J Curr Glaucoma Pr. 2014;8:63–6.
22. Liberati A, Altman DG, Tetzlaff J, Mulrow C, Gøtzsche PC, Ioannidis JP, et al. The PRISMA statement for reporting systematic reviews and meta-analyses of studies that evaluate health care interventions: explanation and elaboration. PLoS Med. 2009;6:e1000100.
23. Rethlefsen ML, Kirtley S, Waffenschmidt S, Ayala AP, Moher D, Page MJ, et al. PRISMA-S: an extension to the PRISMA statement for reporting literature searches in systematic reviews. Syst Rev. 2021;10:39.
24. Lee GA, Hirst LW. Ocular surface squamous neoplasia. Surv Ophthalmol. 1995;39:429–50.
25. Ong SS, Vora GK, Gupta PK. Anterior segment imaging in ocular surface squamous neoplasia. J Ophthalmol. 2016;2016:5435092.
26. Shousha MA, Karp CL, Perez VL, Hoffmann R, Ventura R, Chang V, et al. Diagnosis and management of conjunctival and corneal intraepithelial neoplasia using ultra high-resolution optical coherence tomography. Ophthalmology 2011;118:1531–7.
27. Theotoka D, Morkin MI, Naranjo A, Dubovy SR, Karp CL. Spontaneous regression of ocular surface squamous neoplasia: Possible etiologic mechanisms in cancer resolution. Ocul Surf. 2020;18:351–3.
28. Chin EK, Cortés DE, Lam A, Mannis MJ. Anterior segment OCT and confocal microscopy findings in atypical corneal intraepithelial neoplasia. Cornea 2013;32:875–9.
29. Vempuluru VS, Ghose N, Vithalani NM, Sultana S, Kaliki S. Spontaneous regression of presumed ocular surface squamous neoplasia: A report of 8 cases. Eur J Ophthalmol. 2022;32:3029–34.
30. Joag MG, Gupta A, Galor A, Dubovy SR, Bermudez-Magner JA, Wang J, et al. Conjunctival intraepithelial neoplasia with mucoepidermoid differentiation: A case report of a subtle lesion. Ocul Oncol Pathol. 2015;1:278–82.
31. Tran AQ, Venkateswaran N, Galor A, Karp CL. Utility of high-resolution anterior segment optical coherence tomography in the diagnosis and management of sub-clinical ocular surface squamous neoplasia. Eye Vis. 2019;6:27.
32. Aboumourad RJ, Galor A, Karp CL. Case series: High-resolution optical coherence tomography as an optical biopsy in ocular surface squamous neoplasia. Optom Vis Sci. 2021;98:450–5.
33. Singh S, Mittal R, Ghosh A, Tripathy D, Rath S. High-resolution anterior segment optical coherence tomography in intraepithelial versus invasive ocular surface squamous neoplasia. Cornea 2018;37:1292–8.
34. Vempuluru VS, Jakati S, Godbole A, Mishra DK, Mohamed A, Kaliki S. Spectrum of AS-OCT features of ocular surface tumors and correlation of clinico-tomographic features with histopathology: a study of 70 lesions. Int Ophthalmol. 2021;41:3571–86.
35. Yim M, Galor A, Nanji A, Joag M, Palioura S, Feuer W, et al. Ability of novice clinicians to interpret high-resolution optical coherence tomography for ocular surface lesions. Can J Ophthalmol. 2018;53:150–4.
36. Medina CA, Plesec T, Singh AD. Optical coherence tomography imaging of ocular and periocular tumours. Br J Ophthalmol. 2014;98:ii40–ii46.
37. Thomas BJ, Galor A, Nanji AA, El Sayyad F, Wang J, Dubovy SR, et al. Ultra high-resolution anterior segment optical coherence tomography in the diagnosis and management of ocular surface squamous neoplasia. Ocul Surf. 2014;12:46–58.
38. Vajzovic LM, Karp CL, Haft P, Shousha MA, Dubovy SR, Hurmeric V, et al. Ultra high-resolution anterior segment optical coherence tomography in the evaluation of anterior corneal dystrophies and degenerations. Ophthalmology 2011;118:1291–6.
39. Nanji AA, Sayyad FE, Galor A, Dubovy S, Karp CL. High-resolution optical coherence tomography as an adjunctive tool in the diagnosis of corneal and conjunctival pathology. Ocul Surf. 2015;13:226–35.
40. Atallah M, Joag M, Galor A, Amescua G, Nanji A, Wang J, et al. Role of high-resolution optical coherence tomography in diagnosing ocular surface squamous neoplasia with coexisting ocular surface diseases. Ocul Surf. 2017;15:688–95.
41. Kieval JZ, Karp CL, Abou Shousha M, Galor A, Hoffman RA, Dubovy SR, et al. Ultra-high resolution optical coherence tomography for differentiation of ocular surface squamous neoplasia and pterygia. Ophthalmology 2012;119:481–6.
42. Lozano García I, Romero Caballero MD, Sellés Navarro I. High resolution anterior segment optical coherence tomography for differential diagnosis between corneo-conjunctival intraepithelial neoplasia and pterygium. Arch Soc Esp Oftalmol. 2020;95:108–13.
43. Shousha MA, Karp CL, Canto AP, Hodson K, Oellers P, Kao AA, et al. Diagnosis of ocular surface lesions using ultra-high-resolution optical coherence tomography. Ophthalmology 2013;120:883–91.
44. Karp CL, Mercado C, Venkateswaran N, Ruggeri M, Galor A, Garcia A, et al. Use of high-resolution optical coherence tomography in the surgical management of ocular surface squamous neoplasia: A pilot study. Am J Ophthalmol. 2019;206:17–31.
45. Elhamaky TR, Elbarky AM. AS-OCT guided treatment of diffuse conjunctival squamous cell carcinoma with resection, amniotic membrane graft and topical mitomycin C. Clin Ophthalmol. 2019;13:2269–78.

46. García de Oteyza G, Vázquez-Romo KA, Garcia-Vazquez R, Bermúdez-Cobos D, Ramos-Betancourt N. Complete regression of a giant conjunctival intraepithelial neoplasia using 5-fluorouracil. J Fr Ophtalmol. 2019;42:666–7.
47. Sun Y, Hua R. Long-term efficacy and safety of subconjunctival/perilesional 5-fluorouracil injections for ocular surface squamous neoplasia. Drug Des Devel Ther. 2020;14:5659–65.
48. Füst Á, Tóth J, Imre L, Nagy ZZ. Non-malignant conjunctival epithelial masses with ocular surface squamous neoplasia-like optical coherence tomography features. Int Ophthalmol. 2021;41:1827–34.
49. Arya D, Das S, Gandhi A. Ipsilateral presentation of ocular surface squamous neoplasia and conjunctival melanoma in xeroderma pigmentosum: A rare occurrence. Indian J Ophthalmol. 2019;67:2068–71.
50. Adler E, Turner JR, Stone DU. Ocular surface squamous neoplasia: a survey of changes in the standard of care from 2003 to 2012. Cornea 2013;32:1558–61.
51. Bolek B, Wylęgała A, Teper S, Kokot J, Wylęgała E. Treatment of conjunctival papilloma with topical interferon alpha-2b—case report. Medicine 2020;99:e19181.
52. Kaliki S, Maniar A, Jakati S, Mishra DK. Anterior segment optical coherence tomography features of pseudoepitheliomatous hyperplasia of the ocular surface: a study of 9 lesions. Int Ophthalmol. 2021;41:113–9.
53. Kawabata S, Yoshikawa Y, Kurisu Y, Tajiri K, Kida T, Hirose Y. Conjunctival epithelial hyperplasia in a patient with a nodular lesion in the palpebral conjunctiva: A case report. Biomed Rep. 2022;16:24.
54. Shields CL, Shields JA. Tumors of the conjunctiva and cornea. Indian J Ophthalmol. 2019;67:1930–48.
55. Folberg R, McLean IW, Zimmerman LE. Primary acquired melanosis of the conjunctiva. Hum Pathol. 1985;16:129–35.
56. Shields CL, Fasiuddin AF, Mashayekhi A, Shields JA. Conjunctival nevi: clinical features and natural course in 410 consecutive patients. Arch Ophthalmol. 2004;122:167–75.
57. Shields CL, Shields JA, Gündüz K, Cater J, Mercado GV, Gross N, et al. Conjunctival melanoma: risk factors for recurrence, exenteration, metastasis, and death in 150 consecutive patients. Arch Ophthalmol. 2000;118:1497–507.
58. Kujala E, Tuomaala S, Eskelin S, Kivelä T. Mortality after uveal and conjunctival melanoma: which tumour is more deadly? Acta Ophthalmol. 2009;87:149–53.
59. Shields CL, Belinsky I, Romanelli-Gobbi M, Guzman JM, Mazzuca D Jr, Green WR, et al. Anterior segment optical coherence tomography of conjunctival nevus. Ophthalmology 2011;118:915–9.
60. Shields CL, Regillo AC, Mellen PL, Kaliki S, Lally SE, Shields JA. Giant conjunctival nevus: clinical features and natural course in 32 cases. JAMA Ophthalmol. 2013;131:857–63.
61. Vizvári E, Skribek Á, Polgár N, Vörös A, Sziklai P, Tóth-Molnár E. Conjunctival melanocytic naevus: Diagnostic value of anterior segment optical coherence tomography and ultrasound biomicroscopy. PLoS One 2018;13:e0192908.
62. Demirci H, Steen DW. Limitations in imaging common conjunctival and corneal pathologies with Fourier-domain optical coherence tomography. Middle East Afr J Ophthalmol. 2014;21:220–4.
63. Choi CS, Hamrah P, Laver N. Cystic compound melanocytic nevus in a pediatric patient. Ophthalmology 2016;123:2293.
64. Alzahrani YA, Kumar S, Abdul Aziz H, Plesec T, Singh AD. Primary acquired melanosis: Clinical, histopathologic and optical coherence tomographic correlation. Ocul Oncol Pathol. 2016;2:123–7.
65. Liu KC, Mruthyunjaya P, Proia AD, Vora GK. Pediatric conjunctival melanoma arising from a compound nevus. J AAPOS. 2017;21:416–8.
66. Zembowicz A, Mandal RV, Choopong P. Melanocytic lesions of the conjunctiva. Arch Pathol Lab Med. 2010;134:1785–92.
67. Daya SM, Papdopoulos R. Ocular coherence tomography in lymphangiectasia. Cornea 2011;30:1170–2.
68. Gokhale NS. AS-OCT in diffuse conjunctival lymphangiectasia. Indian J Ophthalmol. 2019;67:1338.
69. Swann PG, Han T. Lymphangiectasia. Clin Exp Optom. 2018;10:418–9.
70. Bunod R, Adams D, Cauquil C, Francou B, Labeyrie C, Bourenane H, et al. Conjunctival lymphangiectasia as a biomarker of severe systemic disease in Ser77Tyr hereditary transthyretin amyloidosis. Br J Ophthalmol. 2020;104:1363–7.
71. Volek E, Toth J, Nagy ZZ, Schneider M. Evaluation of lymphatic vessel dilatations by anterior segment swept-source optical coherence tomography: case report. BMC Ophthalmol. 2017;17:194.
72. Han KE, Choi CY, Seo KY. Removal of lymphangiectasis using high-frequency radio wave electrosurgery. Cornea 2013;32:547–9.
73. Choi SM, Jin KH, Kim TG. Successful treatment of conjunctival lymphangiectasia accompanied by corneal dellen using a high-frequency radiowave electrosurgical device. Indian J Ophthalmol. 2019;67:409–11.
74. Goshe JM, Platt S, Yeaney G, Singh AD. Surgical drainage of lymphangiectasia haemorrhagica conjunctivae. Cornea 2017;36:116–8.
75. Welch J, Srinivasan S, Lyall D, Roberts F. Conjunctival lymphangiectasia: a report of 11 cases and review of literature. Surv Ophthalmol. 2012;57:136–48.
76. Bekdemir Ş, Gündüz AK, Ataoğlu Ö. Ipsilateral lymphatic and venous malformations affecting the midface area. Case Rep Ophthalmol Med. 2020;2020:2845035.
77. Bradfield Y, Burkat CN, Albert DM, Potter HAD. Capillary hemangioma presenting as a scleral vascular lesion in a child. Ophthalmic Plast Reconstr Surg. 2019;35:e115–e116.
78. Zein M, Theotoka D, Wall S, Galor A, Cabot F, Patel U, et al. Silk suture granuloma 37 years after scleral buckle surgery: A case report. Cornea 2021;40:1357–9.
79. Jung JJ, Della Torre KE, Fell MR, Teng CC, Freund KB. Presumed pyogenic granuloma associated with intravitreal anti-vascular endothelial growth factor therapy. Open Ophthalmol J. 2011;5:59–62.
80. Gulyesil FF, Dogan M, Sabaner MC, Gobeka HH. How traumatic is intravitreal Ozurdex injection? Ocul Immunol Inflamm. 2021;29:1–3.
81. Venkateswaran N, Mercado C, Tran AQ, Garcia A, Diaz PFM, Dubovy SR, et al. The use of high resolution anterior segment optical coherence tomography for the characterization of conjunctival lymphoma, conjunctival amyloidosis and benign reactive lymphoid hyperplasia. Eye Vis. 2019;6:17.
82. Koay AC, Wong KT, Subrayan V. Benign reactive lymphoid hyperplasia affecting both the conjunctiva and the cornea. Graefes Arch Clin Exp Ophthalmol. 2012;250:775–7.
83. Klavdianou O, Kondylis G, Georgopoulos V, Palioura S. Bilateral benign reactive lymphoid hyperplasia of the conjunctiva: a case treated with oral doxycycline and review of the literature. Eye Vis. 2019;6:26.
84. Mirzayev I, Gündüz AK, Cansiz Ersöz C, Gündüz ÖÖ, Gahramanli Z. Anterior segment optical coherence tomography, in vivo confocal microscopy, histopathologic, and immunohistochemical findings in a patient with multiple endocrine neoplasia type 2b. Ophthalmic Genet. 2020;41:491–6.
85. Chang TC, Okafor KC, Cavuoto KM, Dubovy SR, Karp CL. Pediatric multiple endocrine neoplasia type 2b: Clinicopathological correlation of perilimbal mucosal neuromas and treatment of secondary open-angle glaucoma. Ocul Oncol Pathol. 2018;4:196–8.
86. Alvarado-Villacorta R, Davila-Alquisiras JH, Ramos-Betancourt N, Vazquez-Romo KA, Hernández-Ayuso I, Ríos Y et al. Conjunctival myxoma: High-resolution optical coherence tomography findings of a rare tumor. Cornea 2022;41:1049–52
87. Østergaard J, Prause JU, Heegaard S. Oncocytic lesions of the ophthalmic region: a clinicopathological study with emphasis on cytokeratin expression. Acta Ophthalmol. 2011;89:263–7.
88. Say EA, Shields CL, Bianciotto C, Eagle RC Jr, Shields JA. Oncocytic lesions (oncocytoma) of the ocular adnexa: report of 15 cases and review of literature. Ophthalmic Plast Reconstr Surg. 2012;28:14–21.
89. Soliman W, Mohamed TA. Spectral domain anterior segment optical coherence tomography assessment of pterygium and pinguecula. Acta Ophthalmol. 2012;90:461–5.
90. Shifera AS, Eberhart C, Kuo IC. Role of anterior segment imaging in the diagnosis of atypical pterygium. Can J Ophthalmol. 2020;55:e115–e117.
91. Lluch S, Julio G, Pujol P, Merindano D. What biomarkers explain about pterygium OCT pattern. Graefes Arch Clin Exp Ophthalmol. 2016;254:143–8.
92. Pujol P, Julio G, Barbany M, Asaad M. Healing indicators after pterygium excision by optical coherence tomography. Ophthalmic Physiol Opt. 2015;35:308–14.
93. Gasser T, Romano V, Seifarth C, Bechrakis NE, Kaye SB, Steger B. Morphometric characterisation of pterygium associated with corneal stromal scarring using high-resolution anterior segment optical coherence tomography. Br J Ophthalmol. 2017;101:660–4.
94. Raj A, Dhasmana R, Bahadur H. Morphometric evaluation and measurements of primary pterygium by anterior segment optical coherence tomography and its relation with astigmatism. Ther Adv Ophthalmol. 2021;13:25158414211020145.
95. Minami K, Tokunaga T, Okamoto K, Miyata K, Oshika T. Influence of pterygium size on corneal higher-order aberration evaluated using anterior-segment optical coherence tomography. BMC Ophthalmol. 2018;18:166.
96. Song H, Rand GM, Kwon JW. Clinical features of pingueculitis revealed by anterior segment optical coherence tomography findings. Eye Contact Lens. 2019;45:394–8.
97. Ahn SJ, Shin KH, Kim MK, Wee WR, Kwon JW. One-year outcome of argon laser photocoagulation of pinguecula. Cornea 2013;32:971–5.
98. Nahon-Estève S, Martel A, Maschi C, Baillif S, Lassalle S, Caujolle JP. Swept-source and spectral-domain OCT imaging of conjunctival tumors. Ophthalmology 2021;128:947–50.
99. Bianciotto C, Shields CL, Guzman JM, Romanelli-Gobbi M, Mazzuca D Jr, Green WR, et al. Assessment of anterior segment tumors with ultrasound biomicroscopy versus anterior segment optical coherence tomography in 200 cases. Ophthalmology 2011;118:1297–302.

100. Lauwers N, Janssens K, Mertens M, Mathysen D, Lammens M, de Keizer RJW, et al. Anterior segment optical coherence tomography and ultrasound biomicroscopy for measuring thickness of corneal and bulbar conjunctival tumours. Br J Ophthalmol. 2022;106:760–4.
101. Janssens K, Mertens M, Lauwers N, de Keizer RJ, Mathysen DG, De Groot V, et al. To study and determine the role of anterior segment optical coherence tomography and ultrasound biomicroscopy in corneal and conjunctival tumors. J Ophthalmol. 2016;2016:1048760.

ACKNOWLEDGEMENTS

All pathology images except Fig. 3C were obtained by the digital pathology systems supported by Ankara University (AU BAP A140230003). Figure 3C was provided by Private Mikro-Pat Pathology Laboratory, Ankara, Turkey.

AUTHOR CONTRIBUTIONS

All authors contributed to design of the study, data collection, analysis, interpretation, and writing of the paper. AKG and IM were responsible for the literature search and initial preparation of the manuscript. AKG, IM, and ÖÖG collected and interpreted optical coherence tomography images. AOH, IK, ZG, CCE, and ÖA were responsible for obtaining and interpreting pathological images.

COMPETING INTERESTS

The authors declare no competing interests.

ADDITIONAL INFORMATION

Correspondence and requests for materials should be addressed to Ahmet Kaan Gündüz.